IEEE Access
Multidisciplinary ⋮ Rapid Review ⋮ Open Access Journal

Received January 24, 2020, accepted February 2, 2020, date of publication February 10, 2020, date of current version February 18, 2020.

Digital Object Identifier 10.1109/ACCESS.2020.2972766

An Extremum Approximation ARAIM Algorithm Based on GPS and BDS

XIYAN SUN[1,2], LINZHU XU[1], YUANFA JI[1,2], WENTAO FU[1], SUQING YAN[1], AND QIDONG CHEN[3]

[1]Guangxi Key Laboratory of Precision Navigation Technology and Application, Guilin University of Electronic Technology, Guilin 541004, China
[2]National and Local Joint Engineering Research Center of Satellite Navigation and Location Service, Guilin 541004, China
[3]Key Laboratory of Radio Wave Environment and Modeling Technology, Qingdao 266000, China

Corresponding author: Yuanfa Ji (jiyuanfa@163.com)

This work was supported in part by the IGS, MGEX in providing the Multi-GNSS Data, in part by the National Key Research and Development Program of China under Grant 2018YFB0505103, in part by the National Natural Science Foundation of China under Grant 61561016 and Grant 61861008, in part by the funding of the Science and Technology Major Project of Guangxi under Grant AC16380014, Grant AA17202048, and Grant AA17202033, in part by the Natural Science Foundation of Guangxi under Grant 2018JJA170090, in part by the Guilin Science and Technology Bureau Project under Grant 20170216, and in part by the 2019 Innovation Project of GUET Graduate Education under Grant 2019YCXS024.

ABSTRACT Advanced receiver autonomous integrity monitoring (ARAIM) is a new technology that can reduce the vertical protection level (VPL) by optimizing the probability of configuration information to improve availability. Compared with traditional receiver autonomous integrity monitoring (RAIM), the powerful vertical guidance capability of ARAIM highlights its advantages. This paper improves ARAIM performance by reducing the difference between the two most important view solutions affecting the VPL and the all-in-view solution while satisfying the accuracy. First, this paper proposes new constellation configurations suitable for GPS/BDS, which is a nontraditional constellation itself; second, this paper proposes a method called EA-ARAIM for improving ARAIM performance. The results show that for the depleted constellation in the case of visible satellite reduction, the coverage can increase from 59.97% to 76.63% with the assistance of EA-ARAIM. Even for the optimistic constellation, where there is not much room to improve availability, the improved algorithm can increase the coverage to approximately 3%. Finally, compared with the simulation data used in most of the literature, this paper uses real data obtained from MGEX for analysis.

INDEX TERMS ARAIM, GPS and BDS, new constellation configurations, EA-ARAIM, coverage.

I. INTRODUCTION

Due to the increase in the Global Navigation Satellite System (GNSS) constellation, not only GPS, but also BDS, GALILEO and GLONASS are playing increasingly greater roles in global navigation services. More constellations mean that more visible satellites can be used for positioning, which greatly improves geometry [1], [2]. In this way, the accuracy of positioning is obviously improved. In addition, with more frequencies being opened, which can eliminate most ionospheric errors (the largest source of error in pseudorange residuals) with dual-frequency, advanced RAIM has been proposed to replace traditional RAIM [3]. In ARAIM, the combination of multifrequency and multiconstellation greatly improves global vertical guidance [4]. Both are based on an aerial comparison of the consensus of a satellite with those of other visible satellites. However, ARAIM is capable of supporting vertical guidance below 200 feet (LPV-200) relative to RAIM, which only supports LNAV guidance, in line with the development of well service performance. However, this development was accompanied by a more conservative threat model that is needed by ARAIM. The model, combined with weak geometries, results in large position error boundaries and loss of vertical guidance availability [5], [6]. However, the ARAIM concept is actually not fragile; on the contrary, aviation will benefit from it and will not be sensitive to negative changes in the underlying constellation.

ARAIM is designed to achieve global coverage of an accurate approach and is first presented in a report published by the GNSS Evolutionary Architecture Study (GEAS); the report initially describes the basic architecture underlying the algorithms of ARAIM and makes the most basic judg-

The associate editor coordinating the review of this manuscript and approving it for publication was Venkata Ratnam Devanaboyina.

ment on the availability of ARAIM [4]. Subsequently, literature [7]–[9] provide a more detailed explanation of the algorithm and simultaneously conducts more detailed research on some cases; a major section compares the coverage of the ARAIM algorithm with a depleted constellation, nominal constellation and optimistic constellation, and the online and offline forms are described. However, these reports are based on the two constellations, GPS/GALILEO, and the applicability of BDS is basically not mentioned. In addition, most of these studies are based on simulation data and lack ARAIM applicability and improved performance of GPS/BDS [10], [11].

The BDS consists of 30 satellites, including 3 geosynchronous orbit satellites (GEOs), 3 inclined geosynchronous orbit satellites (IGSOs), 24 medium-earth orbiting satellites (MEOs) and some in-orbit spare satellites [12]; the BeiDou constellation is the most applicable to the Asia-Pacific region, so we use the ARAIM algorithm based on the two major constellations of BDS/GPS to evaluate the performance of ARAIM in the Asia-Pacific region.

The basic ARAIM algorithm is introduced in [3]. In addition, improvement in the false alarm risk distribution, improvement in the threat model and improvement in the position solution have been proposed to improve the performance of the ARAIM algorithm. These studies can enlighten the relevant workers, such as literature [13], [14], which have made great contribution to the development of ARAIM. Admittedly, improvement in ARAIM performance is a major problem and would allow ARAIM to provide well services to the world. The classic method is to obtain a series of parameters by least squares to evaluate RAIM. This method provides an optimal solution for the accuracy under nominal conditions. However, the protection level is not necessarily optimal, so we can apply the method of changing the position solution to optimize the protection level [15]. This concept is called the non-least-squares (NLS) estimation. This method has been exploited in NIORAIM's slope-based RAIM framework [16], which uses the weighting method to change the position solution to obtain optimal accuracy and integrity [16], [17]. In this way, the availability of the algorithm has been greatly increased and can provide great integrity monitoring even in the event of a serious constellation malfunction. This method has great applicability to the ARAIM algorithm and can be introduced into the ARAIM algorithm to obtain the optimal protection level. In [15], NLS estimation is used to optimize the integrity allocation and the location solution obtained by more constraints, the problem is transformed into a convex optimization problem to obtain a satisfactory protection level, and the original algorithm is carried out. The effect is good, but the number of iterations is too large and the degree of the calculation is quite complicated.

Literature [18] improves the algorithm by combining the fault view solution of the largest variance in the vertical direction with the all-in-view solution. A new optimal all-in-view solution is obtained by the constraint of precision. However, this method only considers the solution with the largest fault. Although simple, in some cases, other fault modes also contribute greatly to the risk of integrity. So this method has certain limitations. Literature [19] provides an optimization method, that uses the difference between the fault mode and the all-in-view solution as the weight, but this method ignores the case that when the fault mode itself meets the conditions in Section IV, the weight of the difference is often not optimal, sometimes resulting in an unsatisfying final result.

It is generally known that the calculation of the protection level often depends on the worst geometry; furthermore, the worst geometry is often due to a fault in the constellation, so this paper proposes an approach based on a weighting method that depends on two maximum values. Thus, an optimal all-in-view solution can be obtained to greatly improve the availability of the ARAIM algorithm while ensuring that all the requirements are met.

II. PERFORMANCE REQUIREMENTS OF THE LPV-200

At present, the ARAIM user algorithm is mostly a multi-hypothesis solution separation (MHSS) ARAIM that configures a probability of hazardously misleading information (PHMI) to perform various aspects of the calculation. The vertical and horizontal guidance that ARAIM can provide for an accurate approach is closely related to the determination of threat models, strongly relying on the assumption of the probability of fault and the maximum magnitude of measurement error that may not be discovered. The more satellites and constellations that are used in the algorithm, the more threat models need to be considered.

A. LPV-200 BASIC REQUIREMENTS

Life safety services aims at quickly detect faults and provide services for critical transportation applications such as aviation safety [4]. Previously, the required positioning accuracy and integrity were primarily provided by satellite-based augmentation systems (SBAS) or ground-based augmentation systems (GBAS). The LPV-200 is a relatively new operation that refers to a vertical guiding process with an approach altitude of 200 feet [4]. Currently, LPV-200 is mainly provided by SBAS, but ARAIM is different from SBAS. The inflation requires a system-specific safety analysis that demonstrates that the performance remains bounded within the same operationally driven limits as information for lateral spacing (ILS). To guarantee this performance, main requirements have been derived:

- 4m 95% accuracy in line with current ICAO Annex 10 requirements for GNSS [17];
- 10 m fault-free accuracy performance at the 10^{-7} level, used to ensure that normal performance will be within ILS look-alike (vertical) limits;
- 15 m effective monitoring threshold (EMT) designed to put a 10^{-5} confidence bound on the maximum error in the vertical dimension;

- Protection levels (PLs):
  $VPL < VAL = 35\ m \& HPL < HAL = 40\ m$
- Probability of False Alarm (P_{fa}) and PHMI:
  $P_{fa} < 4 \times 10^{-6}/15s, PHMI < 2 \times 10^{-7}/approach$

It finds out that ARAIM and SBAS share high degree of similarity at the conceptual level which lead to the consideration of using the same set of requirements to support Category I approach operations. The evaluation of VPL is the most basic criterion. In fact, for WAAS, other conditions are satisfied while satisfying the VPL requirements, mainly because the WAAS' special fault mode determines the calculation of the above criteria. Therefore, it can also ensure that the accuracy can meet the demand and that the EMT does not exceed the threshold when the VPL is lower than 35 m. Traditionally, the provision of vertical guidance with GNSS has required the use of differential correction systems, and it can be known that ARAIM is calculated using an ionosphere-free combination model of multifrequency, which does not involve differential correction in precisely the way used by SBAS systems, and the differential correction can certainly have higher accuracy. In addition, the error detection method of ARAIM also allows for large pseudorange errors before the fault mode is identified and eliminated. LPV-200 has been provided by SBAS before, so for ARAIM, only ensuring VPL below 35 m cannot guarantee that the other conditions also meet the requirements. Therefore, more conservative constraints are needed to ensure that ARAIM can support LPV-200 operation. Therefore, in order to emulate the performance of existing SBAS, three additional requirements have been derived. And accompanied by the above thresholds, whenever the VPL is met, the horizontal protection level (HPL) is always met.

B. THREAT MODEL

Navigation threats are defined as all possible events that cause a deviation from the real location solution, regardless of whether a particular fault can be identified in one of the navigation systems. Based on the current fault model, events are roughly divided into nominal errors, narrow faults, and wide faults [21]. The narrow faults, which can be called single faults, affect the satellite separately but are not part of the nominal error caused by space or ground segment faults and only affect the navigation signal of one satellite. Wide faults, known as constellation faults, are related errors caused by space or ground segment faults that affect navigation information from multiple satellites. The nominal errors are the errors generated by the system during normal operation and are caused by the system itself, such as satellite clock error, troposphere error, receiver noise, and multipath error. There are available models to eliminate these errors, which basically conform to the mathematical Gauss distribution [7].

The two matrices obtained from the nominal errors are used for computing the integrity and accuracy in subsequent ARAIM user algorithms. Each matrix can be described by a Gaussian distribution and the nominal errors. The nominal errors are obtained by the ISM. Of course, other parameters are provided in the ISM for use in subsequent calculations. The main parameters are as described in Table 1.

TABLE 1. Main parameters in ISM.

Name	Description	Source
$\sigma_{URA,i}$	standard deviation of the clock and ephemeris error of satellite i used for integrity	ISM
$\sigma_{URE,i}$	standard deviation of the clock and ephemeris error of satellite i used for accuracy and continuity	ISM
$b_{nom,i}$	maximum nominal bias for satellite i used for integrity	ISM
$P_{sat,i}$	prior probability of a fault in satellite i per approach	ISM
$P_{const,j}$	prior probability of a fault affecting more than one satellite	ISM

III. ARAIM USER ALGORITHM

The ARAIM algorithm is dedicated to the LPV-200 service, and the concept of the algorithm first appeared in literature [4]. The basic characteristics of the algorithm, the basic calculation method and the feasibility of the algorithm are described, and then the algorithm is improved in literature [7]–[9]. MHSS is the core of the ARAIM algorithm. MHSS obtains the fault model by calculating the maximum number of satellites to be monitored, and then calculates these fault models one by one and compares them with the all-in-view solution to identify and eliminate satellite faults. The parameters obtained in the calculated fault model are subsequently used to calculate the protection level, EMT, and accuracy to evaluate the performance of ARAIM.

A. DETERMINATION OF FAULT MODE

The fault mode is mainly determined according to the parameters provided by the ISM. These parameters are given in Table 1, which mainly uses the constellation prior fault probability and the satellite prior fault probability. The probability of constellation prior fault in ARAIM may be equal to or greater than the probability of satellite prior fault, which is not contradictory because unlike in RAIM, constellation faults and satellite faults in ARAIM are two different types of events and are independent.

First, we calculate the maximum simultaneous fault which defined as $N_{fault,max}$. The algorithm starts from a single satellite fault. When the probability of at least r+1 satellite faults is less than the threshold for the integrity risk, the calculation is stopped. At this time, the smallest r is the largest simultaneous fault we need [22]. The definition of this algorithm is as follows:

$$N_{fault,\max} = \begin{cases} 1 - \sum_{r=0}^{N_{fault,\max}+1} P_r \le P_{fault\_thres} \\ 1 - \sum_{r=0}^{N_{fault,\max}} P_r \ge P_{fault\_thres} \end{cases} \quad (1)$$

When the maximum simultaneous faults are calculated, we can determine the fault mode to be monitored in

this epoch. For example, there are 15 visible satellites and 2 constellations, according to the constellation prior probability of the ISM. The probability of satellite a priori fault is calculated as the maximum simultaneous fault of 2, and the numbers of faults to be monitored at this time are 17 one-event faults and 136 two-event faults.

B. FAULT MODE IDENTIFICATION AND ELIMINATION

After determining the total number of faults to be monitored, it is necessary to identify and eliminate these faults. For each fault hypothesis test, the k-th subset position solution is performed by:

$$\begin{aligned} \hat{x}^{(k)} &= S^{(k)} v \\ S^{(k)} &= \left(G^T M^{(k)} W G\right)^{-1} G^T M^{(k)} W \end{aligned} \tag{2}$$

where, $S^{(k)}$ is also called the projection matrix; v is observed pseudorange; $M^{(k)}$ is an identity matrix ($N_{sat} \times N_{sat}$) with the number of H satellites on the diagonal zeroed out. The indices for the number of H satellites that are zeroed out are defined by the k-th fault mode; G is the observation matrix, consisting of cosine and clock correlation coefficients between the receiver and the satellite; and W is the corresponding weight matrix, determined by $\sigma_{URA,i}$ in the ISM parameter.

Subsequently, the solution separation covariance in the East-North-Up coordinate system, which is defined as $\sigma_{ss,q}^{(k)}$, are calculated as follows:

$$\sigma_{ss,q}^{(k)} = \sqrt{\Delta S_q^{(k)} C_{acc} \Delta S_q^{(k)T}} \tag{3}$$

We use q $= 1, 2,$ and 3 to represent east, north and up, respectively. Different from formula 2, C_{acc} is the matrix to evaluate the accuracy and continuity and based on $\sigma_{URE,i}$ in the ISM parameter, and $\sigma_{ss,q}^{(k)}$ is used to calculate the detection threshold of the k-th fault mode. The detection threshold is calculated as follows:

$$T_{k,q} = K_{fa,q} \sigma_{ss,q}^{(k)} \tag{4}$$

where, $K_{fa,q}$ is the scale factors which allocated equally to the $N_{faultmodes}$-number of monitored subsets corresponding to the horizontal and vertical dimension and are given by:

$$\begin{aligned} K_{fa,1} &= K_{fa,2} = Q^{-1}\left(\frac{P_{FA\_HOR}}{4N_{faultmodes}}\right) \\ K_{fa,3} &= Q^{-1}\left(\frac{P_{FA\_VERT}}{2N_{faultmodes}}\right) \end{aligned} \tag{5}$$

P_{FA_HOR} is the continuous budget allocation in the horizontal mode, and similarly, P_{FA_VERT} is the continuous budget allocation in the vertical mode. Q is the right cumulative distribution function (cdf) of the normal distribution. Q^{-1} is the inverse of Q. Subsequently, we conduct the following tests:

$$\left|\hat{x}_q^{(k)} - \hat{x}_q^{(0)}\right| \le T_{k,q} \tag{6}$$

If any of the tests fails, exclusion must be attempted.

C. ARAIM ALGORITHM AVAILABILITY CALCULATION

When all of the above tests are passed, the availability calculation of ARAIM algorithm begins. The availability criteria are explained in Section II. The protection level is divided into VPL and HPL. Because the ARAIM algorithm has higher requirements in the vertical direction. Here we take the VPL as an example, and HPL is similar. The final results of VPL, HPL, and EMT are presented through coverage. More intuitive results can be obtained from literature [13], which can indicate why we use the VPL as an example in the following.

The VPL satisfies the following equation:

$$\begin{aligned} 2Q\left(\frac{VPL - b_3^{(0)}}{\sigma_3^{(0)}}\right) + \sum_{k=1}^{N_{faultmodes}} p_{fault,k} \\ \times Q\left(\frac{VPL - T_{k,3} - b_3^{(k)}}{\sigma_3^{(k)}}\right) = PHMI \end{aligned} \tag{7}$$

In the above formula:

$$b_3^{(k)} = \sum_{k=1}^{N_{sat}} \left|S_3^k\right| b_{nom,k} \tag{8}$$

$$\sigma_3^{(k)2} = \left(G^T W^{(k)} G\right)_{3,3}^{-1} \tag{9}$$

$\sigma_3^{(k)}$ is the error uncertainty in $\hat{x}^{(k)}$ in the vertical direction. $b_3^{(k)}$ is bias on the range measurements in one dimension for evaluate the integrity. PHMI is the integrity budget that has been allocated.

EMT is defined as the maximum value of the monitoring threshold when the prior fault probability is greater than or equal to P_{EMT},which can be expressed as follows:

$$EMT = \max_{k|p_{fault,k} \ge P_{EMT}} T_{k,3} \tag{10}$$

σ_{acc} is defined as the standard deviation of the all-in-view position solution and is calculated as follows:

$$\sigma_{acc} = \sqrt{S_3^{(0)} C_{acc} S_3^{(0)T}} \tag{11}$$

D. ARAIM ALGORITHM OF EXTREMUM APPROXIMATION

The calculation method that concerns VPL the most in the ARAIM algorithm was given in the previous section. It can be seen that the calculation of VPL has a great correlation with the all-in-view solution, which is also reflected in the existing literature. Particularly, $\sigma_3^{(k)}$ is the parameter inherent in the fault mode. $b_3^{(k)}$ contributes slightly to VPL, whereas $S^{(0)}$ contributes greatly to VPL, HPL and EMT. Therefore, it is feasible to reduce the VPL by adjusting the all-in-view solution. However, it should be noted that the new all-in-view solution should meet the need for accuracy.

We know that the VPL is usually determined by the worst geometry. In the fault modes, we need to set the weight parameter of the corresponding hypothetical faulty satellite to 0, indicating that the satellite does not participate in the positioning. Under constellation faults, all the satellites in the constellation do not participate in the positioning. The more

parameters that are set to 0, the greater potential contribution to VPL. There is an iterative method for calculating VPL in a variety of calculation methods. The expression is as follows:

$$VPL_{low,init} = \max \begin{cases} Q^{-1}\left(\frac{PHMI}{2}\right)\sigma_3^{(0)} + b_3^{(0)} \\ \max\limits_k \; Q^{-1}\left(\frac{PHMI}{p_{fault,k}}\right)\sigma_3^{(k)} + T_{k,3} + b_3^{(k)} \end{cases} \tag{12}$$

$$VPL_{up,init} = \max \begin{cases} Q^{-1}\left(\frac{PHMI}{2\left(N_{faults}+1\right)}\right)\sigma_3^{(0)} + b_3^{(0)} \\ \max\limits_k \; Q^{-1}\left(\frac{PHMI}{p_{fault,k}\left(N_{faults}+1\right)}\right)\sigma_3^{(k)} + T_{k,3} + b_3^{(k)} \end{cases} \tag{13}$$

N_{faults} is equivalent to $N_{faultmodes}$ [3]. The above effect is achieved through two allocation methods to PHMI according to the above formulas. The VPL must be between the upper and lower limits, so this paper proposes a method to reduce the VPL upper and lower limits to reduce the VPL. Weighting the solution containing the two largest faults can also reduce the VPL when other conditions are met. The essence of the algorithm is an OWAS method, which first appeared in literature [17]. Two OWAS methods are proposed in the literature. The application scope of OWAS-1 is not suitable for the ARAIM algorithm. OWAS-2 happens to work together with multiple constellations. The all-in-view solution is replaced by a weighted value of the individual constellation solution to achieve a reduction in the level of protection. In ARAIM, the final VPL value is dependent on all possibilities in the all-in-view. Although the constellation difference is quite large, we cannot ignore the impacts of other subsets of faults. When the VPL of a certain epoch exceeds the threshold value or is too large, it indicates that the geometry is already very poor. At this time, we reallocate $T_{k,3}$ to improve the difference caused by the two worst geometries. We call this EA-ARAIM.

As we know, the all-in-view solution should meet the following criteria [15]:

$$\left(S^{(0)}_{all-in-view} G\right)_{q,q} = 1 \tag{14}$$

The optimal solution to this problem can be computed by extremum approximation. Here, the main ideas of the solution are described:

$$S_3^{(0)new} = (1-k_1-k_2)S_3^{(0)} + k_1 S_3^{(\max 1)} + k_2 S_3^{(\max 2)} \tag{15}$$

Then, we recalculate the parameters we need:

$$\begin{aligned} \Delta S_3^{\max 1} &= (1-k_1)\left(S_3^{(\max 1)} - S_3^{(0)new}\right) \\ &\quad - k_2\left(S_3^{(\max 2)} - S_3^{(0)new}\right) \\ \sigma_{ss,3}^{\max 1} &= \sqrt{\Delta S_3^{(\max 1)} \sigma_{acc} \Delta S_3^{(\max 1)T}} \\ \Delta S_3^{\max 2} &= (1-k_2)\left(S_3^{(\max 2)} - S_3^{(0)new}\right) \\ &\quad - k_1\left(S_3^{(\max 1)} - S_3^{(0)new}\right) \\ \sigma_{ss,3}^{\max 2} &= \sqrt{\Delta S_3^{(\max 2)} \sigma_{acc} \Delta S_3^{(\max 2)T}} \end{aligned} \tag{16}$$

We change notations so that the notations are simpler. Adopting the notations in the example we define (the $VPL_{low,init}$ for example).

$$\begin{aligned} A &= Q^{-1}\left(\frac{PHMI}{p_{fault,\max 1}}\right)\sigma_3^{(\max 1)} + b_3^{(\max 1)} \\ B &= Q^{-1}\left(\frac{PHMI}{p_{fault,\max 2}}\right)\sigma_3^{(\max 2)} + b_3^{(\max 2)} \end{aligned} \tag{17}$$

The problem is then written:

$$\begin{aligned} &minimize\ max\left(A+K_{fa,3}\sigma_{ss,3}^{max1} \quad B+K_{fa,3}\sigma_{ss,3}^{max2}\right) \\ &subject\ to\ \sqrt{S_3^{(0)new} C_{acc} S_3^{(0)newT}} \le \sigma_{acc,req} \end{aligned} \tag{18}$$

In fact, the equation is complex as the process of finding the optimal solution. It is important to notice that we can find a new vector which is approximately the $S_3^{(0)}$. And according to formula (14) we have:

$$S_3^{(0)new} \approx S_{3,new}^{(0)} = t_1 S_3^{(\max 1)} + (1-t_1) S_3^{(\max 2)} \tag{19}$$

We rewrite the problem as:

$$\begin{aligned} \Delta S_3^{\max 1} &= \left((1-k_1)(1-t_1) + t_1 k_2\right)\left(S_3^{(\max 1)} - S_3^{(\max 2)}\right) \\ \sigma_{ss,3}^{\max 1} &= \sqrt{\Delta S_3^{(\max 1)} \sigma_{acc} \Delta S_3^{(\max 1)T}} \\ \Delta S_3^{\max 2} &= \left((1-k_2)t_1 + (1-t_1)k_1\right)\left(S_3^{(\max 2)} - S_3^{(\max 1)}\right) \\ \sigma_{ss,3}^{\max 2} &= \sqrt{\Delta S_3^{(\max 2)} \sigma_{acc} \Delta S_3^{(\max 2)T}} \end{aligned} \tag{20}$$

At this point, the problem has been greatly simplified since there is a strong correlation between $\Delta S_3^{\max 1}$ and $\Delta S_3^{\max 2}$.

Now the problem is to find t such that the constraints are verified:

$$\begin{cases} S_3^{(0)new} = tS^{(\max 1)} + (1-t)S^{(\max 2)} \\ \sigma_{acc,new} = \sqrt{S_3^{(0)new} C_{acc} S_3^{(0)newT}} \le \sigma_{acc,req} \\ 0 \le t \le 1 \end{cases} \tag{21}$$

This is a one-dimensional problem that can be easily solved numerically. The algorithm reduces the upper and lower limits of the VPL. When an accurate VPL is calculated in the last iteration, the $T_{k,3}$ of the satellite fault changes. In fact, the algorithm still cannot optimally allocate $T_{k,3}$ because we use an approximate vector to calculate the equation. But we can still get a satisfactory result. The ARAIM algorithm runs every epoch; for higher efficiency, EA-ARAIM is enabled when the baseline ARAIM algorithm cannot meet the performance of LPV-200. The EA-RAIM algorithm reallocates $T_{k,3}$. This reallocation definitely results in a smaller $T_{k,3}$ for a certain fault mode. It is possible to meet the condition which will exclude the satellites represented by this fault mode according to the principle of satellite exclusion (Formula (6)).

TABLE 2. ARAIM performance and constellation structure.

σ_{URA} (m)	σ_{URE} (m)	P_{sat}	P_{const}	b_{nom} (m)	constellation
0.75	$\frac{2}{3}\sigma_{URA}$	10^{-5}	10^{-4}	0.75	Optimistic constellation: the mask angle is 5° (BDS 27) Basic constellation: the mask angle is 10° (BDS 24) Depleted constellation: the mask angle is 15° (BDS 23)
1.0					
1.5					

Even in our test, this circumstance did not occur. If this happens with the constellation fault mode, it will cause a terrible situation that a certain constellation will not participate in positioning, then resulting in a large deviation in the positioning results. Therefore, when the basic algorithm of the ARAIM user is available, the improved algorithm is not used, and when using the EA-ARAIM, if the satellite fault occurs again, even if the probability is small, the algorithm needs to be abandoned in this epoch. However, this will not affect the overall performance of EA-ARAIM because this circumstance is very unlikely. It is worth noting that this possibility is not mentioned in other improved ARAIM algorithms.

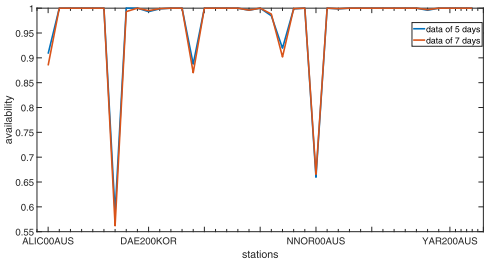

FIGURE 1. Availability of every station based on basic constellation on different days.

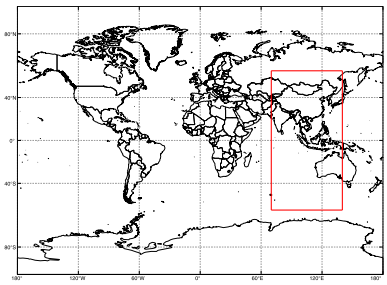

FIGURE 2. Location of the Asia-Pacific region across the map.

IV. SIMULATION AND RESULTS

A. PARAMETER SETTING

In this section, we compare the coverage of the algorithm with the underlying algorithm in the Asia-Pacific region. We use data of 5 days because we use real data; MGEX's station cannot cover the whole grid. In this case, we need to estimate the values of other regions by interpolation. The distribution of the satellite orbit results in strong symmetry of coverage. Therefore, the availability in some areas may be lower than the real availability. For example, the NNOR00AUS station and YAR200AUS station belong to the same area. The availability of the NNOR00AUS station is 66.87%, but the availability of the YAR200AUS station is 100%. Therefore, the deviation in the results obtained from data of 7 days is relatively large. We can obtain this conclusion through Fig. 1. Therefore, we obtain relatively accurate results using data from 5 days. Even the simulations in many literature studies use data from one day. The sampling interval of 10 minutes we select is from the milestone 3 report issued by the ARAIM Technical Subgroup. Therefore, we simulate the grid used for 5 days with an interval of 10 minutes. A total of $336 \times 144 \times 5 = 241920$ points are needed, and coverage means the time available for ARAIM within the grid. The comparison parameters are given in the Table 2.

GPS/BDS is chosen is because this constellation combination has rarely been mentioned and that BeiDou has better performance in the Asia Pacific region than others constellation. And the construction of the BD-3 system is basically completed. The research can also promote the development of BD-3. In this paper, real data are used for evaluating performance of ARAIM, so it is necessary to download observation data and GNSS navigation data from MGEX. Then, we obtain corresponding parameters of ARAIM by receiver. Unlike IGS, MGEX data use the RINEX3 data format, and the observation data can be downloaded from the corresponding stations [23].

In fact, each station of MGEX lists the constellations that can be tracked and has certain coordinates. We evaluate the ARAIM performance of GPS/BDS in the Asia-Pacific region, so we need to select stations in the Asia Pacific region ([70E 140E, 60S 60N]) and have observation data of both GPS and BDS.

Instead of the traditional constellation GPS 24-BDS 24, the depleted constellation GPS 23-BDS 23 and the optimistic constellation GPS 27-BDS 27, the mask angle method is used because when GPS shows poor performance at a monitoring station in the Asia-Pacific region, it does not indicate poor performance in non-Asia-Pacific regions. Therefore, the number of constellation satellites in the traditional sense does not reflect obvious changes in the performance of the algorithm. BDS is composed of MEO, GEO and IGSO, and each has its own characteristics. For example, IGSO can almost only cover the Asia-Pacific region. And this is why we emphasize the Asia Pacific region rather than the worldwide region. Because of this special situation that is different from those of other constellations, we focus on GPS/BDS and propose new constellations configuration for GPS/BDS combination system in the Asia-Pacific region. New constellation configurations contribute to analyzing ARAIM performance. It should be noted that the new constellation configuration is only suitable for analyzing the ARAIM performance of BDS/GPS combination system in the Asia-Pacific region.

TABLE 3. Coverage of basic constellation structure.

algorithm/σ_{URA} (m)	0.75	1	1.5
Baseline algorithm	91.52%	90.32%	84.56%
EA-ARAIM	94.22%	92.01%	89.66%

TABLE 4. Coverage of depleted constellation structure.

algorithm/σ_{URA} (m)	0.75	1	1.5
Baseline algorithm	67.46%	59.97%	44.93%
EA-ARAIM	83.71%	76.63%	59.11%

TABLE 5. Coverage of optimistic constellation structure.

algorithm/σ_{URA} (m)	0.75	1	1.5
Baseline algorithm	91.99%	91.62%	87.07%
EA-ARAIM	94.43%	92.62%	91.65%

B. THREE CONSTELLATION COVERAGE RESULTS AND COMPARATIVE ANALYSIS

The results for the basic constellation coverage are shown in Table 3. The results for the depleted constellation coverage are shown in Table 4. The results for the optimistic constellation coverage are shown in Table 5. In the basic constellation structure, although the coverage decreases as σ_{URA} increases, there is no significant difference in the 99.5% coverage. This trend of change is more evident in the optimistic constellation. The coverage of the basic constellation configuration and the optimistic constellation configuration indicate that the difference in coverage is less than 2%, as shown in Fig. 4. This result shows that although an increase in the mask angle leads to a reduction in the number of satellites, there are enough satellites to meet requirements for precise positioning. At this time, the value of the VPL is mainly related to the geometric distribution of the satellites.

For the depleted constellation, the reduction in the number of visible satellites has a more serious impact on the VPL. The availability under the baseline algorithm is 67.46% when $\sigma_{URA} = 0.75$, Even when $\sigma_{URA} = 1.5$, the availability decreases by nearly 40%. This decrease greatly affects the performance of the ARAIM algorithm. However, with EA-ARAIM, as shown in Fig. 3, most of the coverage areas of 95% and 99% are increased to 99.5%. In this case, life safety services can be well provided with EA-ARAIM.

The coverage of the algorithm for the basic constellation is increased up to about 2%, while that for the optimistic constellation is increased up to only 1%. It seems that the algorithm does not significantly improve the 99.5% coverage. However, it is worth noting that for some regions, the algorithm may increase the coverage by 75% to 95% and increase coverage of 99.5% to 100%. From this, it can be seen that except the certain areas where there is extremely low coverage, the EA-ARAIM can effectively improve the availability loss in other areas. Fig. 1 and Fig. 4 show that there are no coverage areas below 75% because of replacement by other high coverage stations in the area.

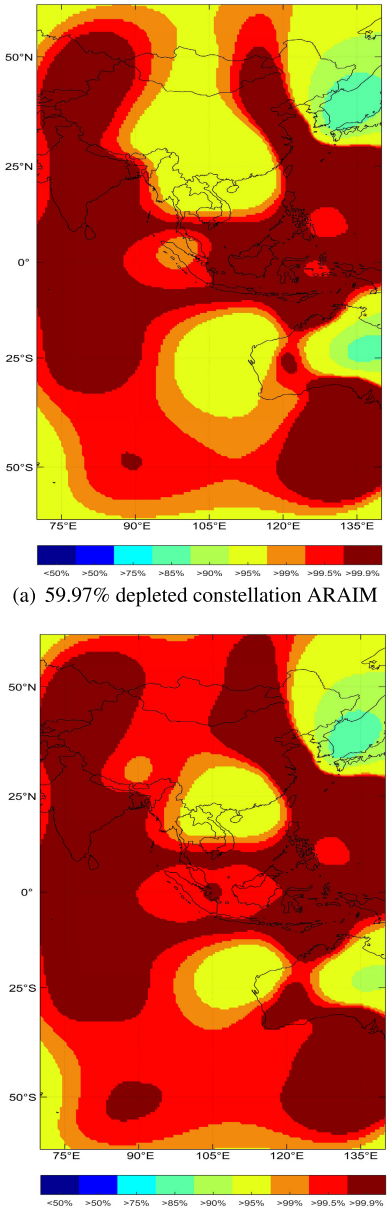

(a) 59.97% depleted constellation ARAIM

(b) 76.63% depleted constellation EA-ARAIM

FIGURE 3. Comparison of coverage of two algorithms for depleted constellation when $\sigma_{URA} = 1$.

The Fig. 5 shows the VPL calculated by two methods for two stations in one day. It can be seen that at the KERG station, the VPL value can be improved to below 35 m. However, at the ALIC station, the threshold value is still exceeded at certain times. Because the poor geometry of the satellites at these time. For these extremely poor geometry, the algorithm can only improve the situation as much as possible. However, the EA-ARAIM cannot completely solve the issue. The σ_{acc} corresponding to the very poor VPL is much larger than the threshold of 1.87, which causes the resulting coefficients t usually do not include the coefficients obtained for the optimal VPL. The value of the coefficient is taken at the boundary where the σ_{acc} is below the threshold.

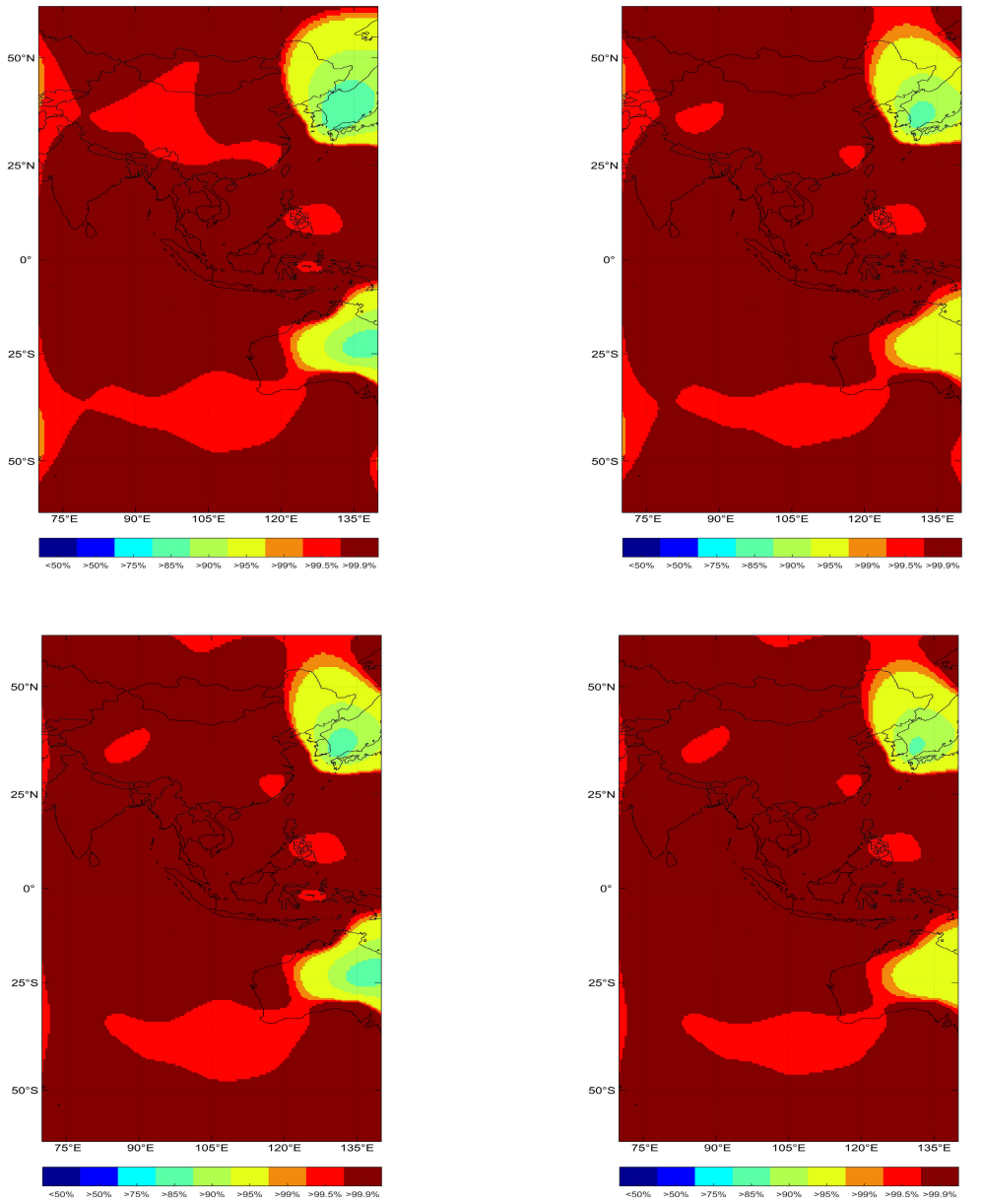

(c) 91.62% optimistic constellation ARAIM

(d) 92.62% optimistic constellation EA-ARAIM

FIGURE 4. **Comparisons between coverage of basic and optimistic constellation when $\sigma_{URA} = 1$.**

Therefore, such an excessive VPL value exceeds the threshold even with EA-ARAIM, which can also explain why there is no change in some of the places where the availability is less than 95% in Fig. 4. In these places, due to terrible geometry, the VPL value of some of the stations is as high as 10^3 m in some epochs. From this, there is no significant increase in areas with coverage greater than 99.5% in above results. And unlike real data, such a situation does not exist in the simulation data. Although the real data is accompanied by various errors, it can well reflect the real ARAIM performance in a certain area. The coverage obtained from the simulation data indicates the best ARAIM performance in a certain area. Therefore, it is reasonable that the above coverage is lower than that of other literatures.

ARAIM can better meet LPV-200 services. At present, the performance of LPV-200 is not fully realized in our country, and ARAIM's low cost and high operability make it possible for ARAIM to replace SBAS in the future, so this technology is crucial. This paper uses GPS/BDS for simulation and analysis of real data and proposes a new constellation structure that can greatly improve the coverage of LPV-200 in our country. EA-ARAIM can also significantly improve coverage. The improvements have an important significance to civil aviation guidance. Especially in areas where the

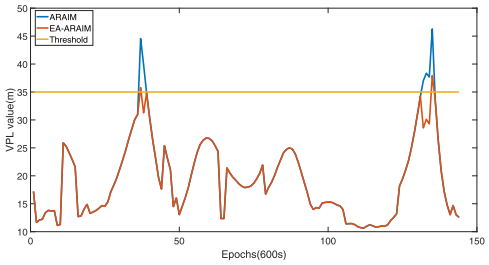

(a) Change in VPL value of ALIC station

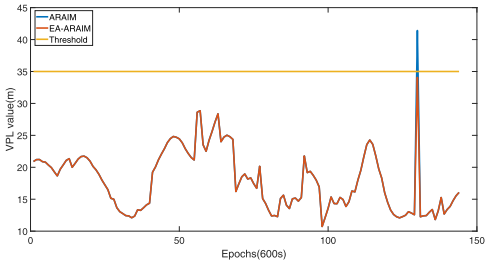

(b) Change in VPL value of KERG station

FIGURE 5. **VPL values of the two algorithms.**

availability is below 90%, EA-ARAIM can increase the availability to a satisfactory range as much as possible. GPS/BDS combination system in the Asia-Pacific region can provide a good guide for the development of BD-3.

V. CONCLUSION

Compared with the traditional GPS/GALILEO constellation used for the evaluation of the performance of ARAIM, this paper proposes a method based on GPS/BDS for the evaluation of the performance of ARAIM in the Asia Pacific region. For the Asia Pacific region, the performance of the BDS constellation is better than that of GPS or GALILEO. On the basis of the above, real data are used for simulation. In addition,the improved algorithm proposed in this paper aims to find the best advantage between the optimal VPL and the accurate value to improve a situation in which the VPL, due to many factors, exceeds the threshold value.

Then, new constellation configurations based on GPS/BDS are proposed because the definition of a constellation structure based in global traditional sense is not suitable for the evaluation of the impact of the structure on the performance of ARAIM in the Asia Pacific region. After the above preparations are performed, the paper compares the influence of three constellation structures and the value of σ_{URA} on the performance of ARAIM and analyzes the significance of the coverage of three constellation structures. Additionally, the EA-ARAIM algorithm is compared with the baseline RAIM algorithm.

Finally,the improved algorithm only works when the VPL exceeds the threshold and is calculated by two inequalities. The complexity of the algorithm does not increase significantly but significantly improves the performance of ARAIM, which highlights the significance of the improved algorithm.

REFERENCES

[1] S. Feng and W. Y. Ochieng, "An Efficient worst user location algorithm for the generation of the galileo integrity flag," *J. Navigat.*, vol. 59, no. 3, pp. 381–394, Sep. 2006.
[2] J. Liu, D. Gu, B. Ju, J. Yao, X. Duan, and D. Yi, "Basic performance of BeiDou-2 navigation satellite system used in LEO satellites precise orbit determination," *Chin. J. Aeronaut.*, vol. 27, no. 5, pp. 1251–1258, Oct. 2014.
[3] J. Blanch, T. Walter, and P. Enge, "Advanced RAIM user algorithm description: Integrity support message processing, fault detection, exclusion, and protection level calculation," in *Proc. ION GNSS*, 2012, pp. 2828–2849.
[4] FAA GEAS Panel. (2010). *Phase II of the GNSS Evolutionary Architecture Study*. [Online]. Available: https://www.faa.gov/about/office_org/headquarters_offices/ato/service_units/techops/navservices/gnss/library/documents/media/GEASPhaseII_Final.pdf
[5] S. Perea, M. Meurer, M. Rippl, B. Belabbas, and M. Joerger, "URA/SISA analysis for GPS and Galileo to support ARAIM," *J. Inst. Navigat.*, vol. 64, no. 2, pp. 237–254, Jun. 2017.
[6] A. El-Mowafy, "Advanced receiver autonomous integrity monitoring using triple frequency data with a focus on treatment of biases," *Adv. Space Res.*, vol. 59, no. 8, pp. 2148–2157, Apr. 2017.
[7] Working Group C. (2013). *ARAIM Technical Subgroup Milestone 1*. [Online]. Available: https://www.gps.gov/policy/cooperation/europe/2013/working-group-c
[8] Working Group C. (2015). *ARAIM Technical Subgroup Milestone 2*. [Online]. Available: https://www.gps.gov/policy/cooperation/europe/2015/working-group-c
[9] Working Group C. (2016). *ARAIM Technical Subgroup Milestone 3*. [Online]. Available: https://www.gps.gov/policy/cooperation/europe/2016/working-group-c
[10] Y. Liu and Y. Zhu, "Design and performance evaluation of airspaceground cooperative GPS/BeiDou dual-constellation RAIM algorithm," in *Proc. ION ITM*, 2014, pp. 127–136.
[11] A. El-Mowafy, "Pilot evaluation of integrating GLONASS, galileo and BeiDou with GPS in araim," *Nephron Clin. Pract.*, vol. 51, no. 1, pp. 31–44, 2016.
[12] China Satellite Navigation Office (CSNO). (2016). *BeiDou Navigation Satellite System Signal in Space Interface Control Document Open Service Signals B1C and B2a*," [Online]. Available: http://www.beidou.gov.cn/xt/gfxz/201712/P020171218337008148266.pdf
[13] Q. Meng, J. Liu, Q. Zeng, S. Feng, and R. Xu, "Improved ARAIM fault modes determination scheme based on feedback structure with probability accumulation," *GPS Solutions*, vol. 23, no. 1, p. 16, 2019.
[14] P. Zhao, Y. Zhu, R. Xue, and L. Zheng, "Parity space projection line based fault detection method for advanced receiver autonomous integrity monitoring," *IEEE Access*, vol. 6, pp. 40836–40845, 2018.
[15] J. Blanch, T. Walter, and P. Enge, "Optimal positioning for advanced RAIM," *J. Inst. Navigat.*, vol. 60, no. 4, pp. 279–289, Dec. 2013.
[16] P. Y. Hwang and C. Colins, "RAIM FDE revisited: A new breakthrough in availability performance with NIORAIM (novel integrity-optimized RAIM)," in *Proc. ION NTM*, San Diego, CA, USA, 2005, pp. 654–665.
[17] Y. C. Lee, "Two new RAIM methods based on the optimally weighted average solution (OWAS) concept," *Navigation*, vol. 54, no. 4, pp. 333–345, Dec. 2007.
[18] J. Blanch, T. Walter, P. Enge, and V. Kropp, "A simple position estimator that improves advanced RAIM performance," *IEEE Trans. Aerosp. Electron. Syst.*, vol. 51, no. 3, pp. 2485–2489, Jul. 2015.
[19] Q. Meng, J. Liu, Q. Zeng, S. Feng, and R. Xu, "Impact of one satellite outage on ARAIM depleted constellation configurations," *Chin. J. Aeronaut.*, vol. 32, no. 4, pp. 967–977, Apr. 2019.
[20] *GNSS Standards and Recommended Practices(SARPs).Section 3.7, Appendix B, and Attachment D, Aeronautical Telecommunications, (Radio Navigation Aids), Amendment 84*, International Civil Aviation Organization (ICAO), Montreal, QC, USA, 2009, vol. 1.
[21] T. Walter, J. Blanch, and P. Enge, "Reduced subset analysis for multi-constellation ARAIM," in *Proc. ION ITM,* San Diego, CA, USA, 2014, pp. 89–98.
[22] Y. Ge, Z. Wang, and Y. Zhu, "Reduced ARAIM monitoring subset method based on satellites in different orbital planes," *GPS Solutions*, vol. 21, no. 4, pp. 1443–1456, Oct. 2017.
[23] O. Montenbruck, P. Steigenberger, L. Prange, Z. Deng, Q. Zhao, F. Perosanz, I. Romero, C. Noll, A. Stürze, G. Weber, R. Schmid, K. MacLeod, and S. Schaer, "The Multi-GNSS Experiment (MGEX) of the International GNSS Service (IGS)–achievements, prospects and challenges," *Adv. Space Res.*, vol. 59, no. 7, pp. 1671–1697, 2017.

XIYAN SUN was born in Shandong, China, in 1973. She received the M.S. degree from the Guilin University of Electronic Technology, in 2002, and the Ph.D. degree in science and engineering from the National Astronomical Observatories, Chinese Academy of Sciences, in 2006. She is currently with the Guangxi Key Laboratory of Precision Navigation Technology and Application, Guilin University of Electronic Technology, to research satellite navigation and signal processing, and also with the National and Local Joint Engineering Research Center of Satellite Navigation and Location Service. She is the author of two books, more than 100 articles, and more than 30 inventions.

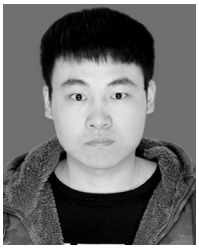

LINZHU XU was born in Shanxi, China, in 1995. He is currently pursuing the master's degree in information and communication engineering with the Guilin University of Electronic Technology and the Research Direction is satellite signal quality monitoring.

YUANFA JI was born Shandong, China, in 1975. He received the M.S. degree from the Guilin University of Electronic Technology, in 2004, and the Ph.D. degree in science and engineering from the National Astronomical Observatories, Chinese Academy of Sciences, in 2008. From 2009 to 2011, he was an Assistant Professor with the Guilin University of Electronic Technology. Since 2012, he has been a Professor with the School of Information and Communication, Guilin University of Electronic Technology. He is also a Professor with the National and Local Joint Engineering Research Center of Satellite Navigation and Location Service and the Guangxi Key Laboratory of Precision Navigation Technology and Application, Guilin University of Electronic Technology. He is the author of one book, more than 100 articles, and more than 30 inventions. His research interests include satellite communications, satellite navigation, real-time kinematic positioning, and navigation receiver.

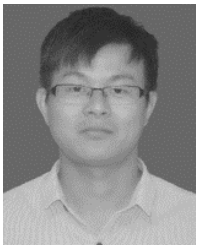

WENTAO FU was born in Henan, China, in 1989. He received the M.S. degree from the Guilin University of Electronic Technology, in 2018. He is currently with the Guangxi Key Laboratory of Precision Navigation Technology and Application, Guilin University of Electronic Technology, to research satellite navigation and signal processing.

SUQING YAN was born in Guangxi, China, in 1975. She received the M.S. degree from the Guilin University of Electronic Technology, in 2005. She has been with the Guangxi Key Laboratory of Precision Navigation Technology and Application, Guilin University of Electronic Technology, to research satellite navigation and signal processing, since 2010. Her research interests include satellite communications, satellite navigation, and signal processing.

QIDONG CHEN was born in Heilongjiang, China, in 1980. He is currently a Senior Engineer with the Key Laboratory of Radio Wave Environment and Modeling Technology. His research interests include radio wave environmental monitoring and radio navigation.